

# Vortex-lattice melting in untwinned $\text{YBa}_2\text{Cu}_3\text{O}_{7-\delta}$ for $H \perp c$

A. Schilling

*Physik-Institut der Universität Zürich, Winterthurerstrasse 190, CH-8057 Zürich, Switzerland*

U. Welp, W. K. Kwok, and G. W. Crabtree

*Materials Science Division, Argonne National Laboratory, Argonne, Illinois 60439*

(Received 10 August 2001; published 3 January 2002)

We have measured the latent heat  $L$  of vortex-lattice melting of optimally doped, untwinned  $\text{YBa}_2\text{Cu}_3\text{O}_{7-\delta}$  as a function of the angle  $\Theta$  between the external magnetic field  $H$  and the crystallographic  $c$  axis. The high resolution in both  $L$  and  $\Theta$  allowed us to explore the configuration with  $H$  perpendicular to  $c$ , where the thermodynamics of the vortex system can be expected to be influenced by the layered structure of the material. Within the resolution of our experiment, we do not detect any deviations of the data from the predictions made by a conventional anisotropic continuum theory. In contrast, continuum-theory expectations are confirmed with high accuracy for magnetic fields that are aligned within  $0.01^\circ$  to the  $b$  axis of the crystal.

DOI: 10.1103/PhysRevB.65.054505

PACS number(s): 74.25.Bt, 74.25.Ha, 74.60.Ge, 75.30.Gw

## I. INTRODUCTION

The thermodynamics of the vortex-lattice melting (VLM) transition in the mixed state of copper-based high-temperature superconductors has been a matter of considerable interest.<sup>1–25</sup> If an external magnetic field  $H$  is not too close to the lower critical field  $H_{c1}$  (Refs. 26,27) and applied parallel to the crystallographic  $c$  axis of a sufficiently clean crystal, the low-temperature vortex phase is a well-ordered lattice with finite elastic constants, leading to zero electrical resistance. As the temperature is increased, the thermal motion of the vortices becomes relevant, and the lattice eventually liquefies at a field-dependent phase boundary.<sup>1–3,27</sup> Beyond a certain magnetic-flux density  $B_{\text{crit,low}}$  [i.e., above a lower critical point in the  $B$ - $T$  phase diagram, the location of which is sample dependent and ranges in  $\text{YBa}_2\text{Cu}_3\text{O}_7$  from  $B_{\text{crit,low}} < 0.1$  up to 4 T (Refs. 17, 20, and 23)], the transition is sharp and of first order with a finite latent heat. The respective solid and fluid phases are not only distinctly different from each other in their spatial symmetry, but also with respect to their response to changes of the external magnetic field or to their reaction to an applied electrical current. The solid phase is magnetically irreversible and has a finite critical-current density, while the fluid phase is reversible and shows zero critical current. Above another limiting flux density  $B_{\text{crit,up}}$  (an upper critical point that may also vary in  $\text{YBa}_2\text{Cu}_3\text{O}_7$  from sample to sample between  $B_{\text{crit,up}} = 9$  T and yet unmeasurably high values<sup>20,23–25,28</sup>), the phase transition becomes less sharp and continuous,<sup>20,25</sup> and the occurrence of magnetic reversibility is no longer necessarily associated with it.<sup>25</sup>

The discontinuous change of thermodynamic quantities at the first-order transition, such as in entropy  $S$  and in magnetization  $M$ , has been measured for  $\text{YBa}_2\text{Cu}_3\text{O}_7$  as a function of magnetic field and temperature,<sup>12–25</sup> and is sufficiently well reproduced by theories.<sup>8,29,30</sup> When the magnetic field is tilted away from the  $c$  axis by a certain angle  $\Theta$ , the melting temperatures  $T_m$  and the discontinuities in  $S$  and  $M$  also depend on  $\Theta$  because of the distinct electronic anisotropy that is common to all cuprate superconductors.<sup>19,21–23</sup> Within an

anisotropic scaling theory for a continuum,<sup>30,31</sup> the melting fields  $H_m(\Theta, T = T_m)$  and the discontinuities  $\Delta S(\Theta)$  and  $\Delta M(\Theta)$  scale in a very transparent way with the corresponding values measured for  $H \parallel c$ , i.e., for  $\Theta = 0$ . This scaling has been experimentally verified to hold in the moderately anisotropic  $\text{YBa}_2\text{Cu}_3\text{O}_7$  for angles up to  $\Theta = 88^\circ$ ,<sup>23</sup> while it fails to explain the data for the highly anisotropic  $\text{Bi}_2\text{Sr}_2\text{CaCu}_2\text{O}_8$  that shows a much more complex vortex-lattice structure in a tilted field.<sup>32,33</sup> However, deviations from continuum-theory expectations may also be expected to occur in  $\text{YBa}_2\text{Cu}_3\text{O}_7$  as soon as  $H$  approaches the  $H \parallel ab$  geometry.<sup>27,34–40</sup> It can be argued that for magnetic fields that are sufficiently closely aligned to the copper-oxygen planes, the vortex lattice accommodates to the crystallographic structure of the material. The resulting highly deformed vortices (Josephson vortices) are expected to show a variety of thermodynamic phases and phase transitions between them that would not be adequately treated in any scaling theory for a continuum.<sup>34–40</sup> For instance, the liquefaction of the low-temperature ordered solid phase to a fluid phase is likely to occur in two steps. A first transition from the ordered solid to an intermediate fluid phase with the long-range order along  $c$  may occur, that eventually melts at a second, higher transition temperature to a fluid state with no long-range order at all. This intermediate-ordered fluid state is very reminiscent to the smectic phases in liquid crystals, where elongated objects are also confined to parallel planes.<sup>38,39</sup>

Early resistivity measurements on untwinned  $\text{YBa}_2\text{Cu}_3\text{O}_7$  single crystals have indeed indicated that the sharp first-order VLM transition is replaced by a smooth crossover as soon as  $H$  is as close as  $0.3^\circ$  to the  $ab$  direction.<sup>41</sup> More recent transport data have revealed clear deviations from conventional angular scaling for the phase-transition fields  $H_m$  near  $H \parallel ab$  in a number of samples.<sup>42</sup> We have, therefore, investigated in detail the  $\Theta$  dependence of the melting temperatures  $T_m$  and the latent heats of melting,  $L = T\Delta S$ , for this geometry. Our strategy is to attempt to treat our data according to conventional anisotropic-scaling schemes, and to search for systematic deviations from such a scaling around  $\Theta = 90^\circ$ .

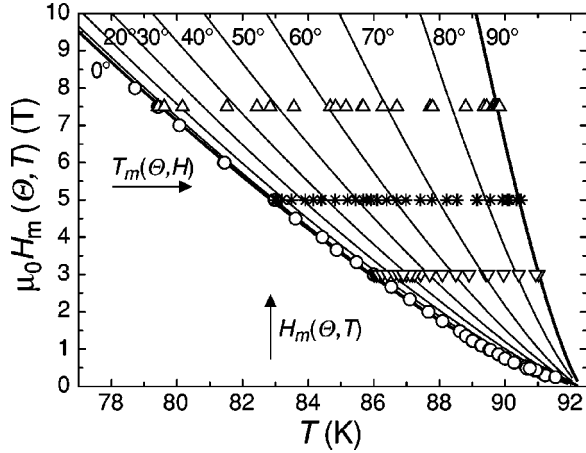


FIG. 1. Magnetic phase diagram of the investigated  $\text{YBa}_2\text{Cu}_3\text{O}_7$  single crystal for varying angle  $\Theta$  between the external magnetic field  $H$  and the crystallographic  $c$  axis. The symbols (circles, triangles, and stars) represent measured VLM melting temperatures  $T_m$ , while the lines have been generated using Eq. (2) with the material parameters given in the main text.

## II. EXPERIMENTAL

We have done a series of 250 heat-capacity measurements for fixed magnetic fields ( $\mu_0 H = 3, 5,$  and  $7.5$  T) and varying  $\Theta$  to study the angular dependence of  $T_m$  and the discontinuity in entropy  $\Delta S$ , and for  $H \parallel c$  and varying  $H$  to obtain a reference data set for the respective angular-scaling analysis (see Fig. 1). The sample is 3.3 mg untwinned  $\text{YBa}_2\text{Cu}_3\text{O}_7$  single crystal with a critical temperature of  $T_c = 92.4$  K. This value is defined by fitting the  $H_m(\Theta = 0^\circ, T)$  vortex-lattice melting line to a power law [see Eq. (4) below], and is in perfect agreement with the position of the peak of the specific heat at the transition to superconductivity in zero magnetic field. The crystal has been previously characterized by heat-capacity and magnetization measurements,<sup>15,18,19,21</sup> and thermodynamic consistency of the respective data has been demonstrated.<sup>15</sup> We used a different type of differential-analysis (DTA) calorimeter with a significantly increased resolution when compared to the apparatus that we had previously used to obtain the data presented in Refs. 15, 18, 19, and 21 (note that due to a recalibration of our thermometers the temperature scale in this work differs by  $+0.4$  K from the scale used in those references). It operates on the basis of the principle described by Schilling and Jeandupeux in Ref. 9, with two calibrated platinum thermometers in a Wheatstone-bridge configuration. Details about the measurement technique will be published elsewhere. The experiment is inserted into a split-coil magnet system (Cryogenics Ltd.) that allows, in principle, for variations in the angle  $\Theta$  of the order of  $0.001^\circ$ . We have checked the accuracy in  $\Theta$  of the combined setup using external laser optics, and we achieve an effective resolution in angle of  $0.01^\circ$ , which is still sufficiently precise for the present investigation. We have calibrated the zero point of the angular scale by carefully monitoring the vortex-lattice melting temperatures for a fixed magnetic field  $H$  around  $\Theta = 90^\circ$  (that corresponds to  $H \parallel b$ ). We have chosen  $\Theta = 90^\circ$  as the angle around which the cor-

responding melting temperatures  $T_m$  show a symmetric dependence on  $\Theta$  (see later in Fig. 3).

## III. RESULTS

### A. The melting temperatures $T_m(\Theta, H)$

For a simple anisotropic scaling of physical properties of copper-oxygen-based superconductors, one may assume that the effective mass  $m^*$  for the current transport can be treated as a tensor.<sup>43</sup> The square root of the ratio of the effective masses along each pair of the three principle axes define three anisotropy ratios, that are, in a general situation, all different from unity. The weak in-plane anisotropy that is of the order of one in the cuprates is often ignored for simplicity, however. In such a uniaxial geometry, where the two crystallographic directions along  $a$  and  $b$  are assumed to be electronically equivalent, only the anisotropy ratio that compares current-transport properties along and perpendicular to the copper-oxygen planes is different from unity. In our experiments we have rotated the magnetic field within the  $bc$  plane. The corresponding relevant anisotropy ratio is, therefore,

$$\gamma_{bc} = \sqrt{m_c^*/m_b^*}, \quad (1)$$

where the indices refer to the respective crystallographic axes. In the following we identify  $\gamma = \gamma_{bc}$  and ignore the in-plane anisotropy that is not further investigated here, although we know from our own thermal investigations on this crystal that  $\gamma_{bc}/\gamma_{ac} = 1.07$  (see Refs. 19, 21, and this paper).

In this simple picture all physical quantities that are related to  $m^*$  (e.g., the magnetic penetration depth  $\lambda$  or the coherence length  $\xi$ ) can be scaled according to the above rules.<sup>43</sup> Along with the scaling of  $\lambda$  and  $\xi$ , one also finds scaling expressions for other derived quantities, such as the lower and the upper critical fields, the elastic constants of the vortex lattice, and the vortex-lattice melting field  $H_m$ .<sup>31</sup> If  $H_m$  is known at a certain fixed temperature  $T$  for  $H \parallel c$ , we expect that the corresponding melting field for an arbitrary angle  $\Theta$  between  $H$  and  $c$  at the same temperature is<sup>31</sup>

$$H_m(T, \Theta) = f(\Theta) H_{m0}(T), \quad (2)$$

where

$$f(\Theta) = \frac{\gamma}{\sqrt{\sin^2(\Theta) + \gamma^2 \cos^2(\Theta)}} \quad (3)$$

(see Fig. 1). This general results does not depend on assumptions about the temperature dependence of  $H_m$ . If an experiment is done at a fixed value of  $H$  and for varying  $\Theta$ , however, the melting temperature  $T_m$  will depend on  $\Theta$  (Fig. 1, horizontal arrow). A formula for  $T_m(\Theta)$  can be given only if we have an expression for the  $T$  dependence of  $H_m$  for any geometry, e.g., for  $H \parallel c$ . Numerous experimental and theoretical works<sup>2-6,12-25</sup> suggests that we have with high precision for  $H \parallel c$  near  $T_c$

$$H_m(T) = H_{m0}(1 - T/T_c)^n. \quad (4)$$

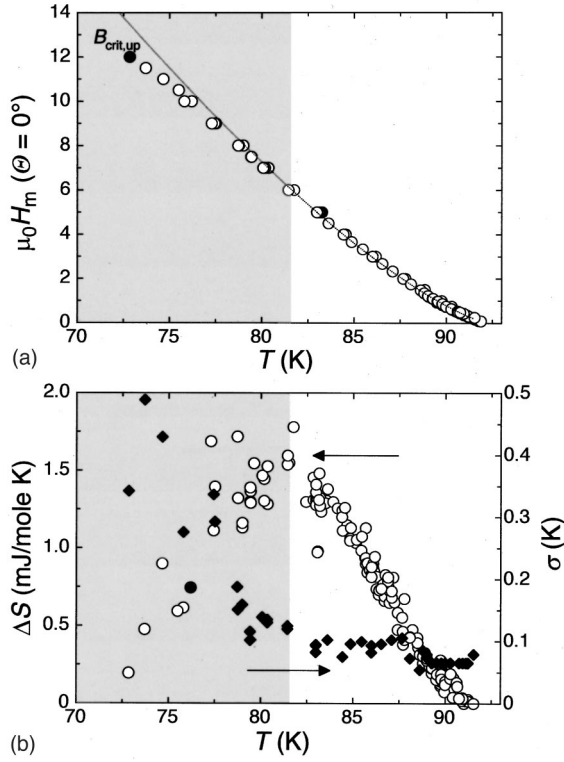


FIG. 2. (a) Experimentally determined phase diagram for  $H \parallel c$  in magnetic fields up to 14 T. In the white region above  $T = 82.5$  K, the  $T$  dependence of  $H_m$  follows almost perfectly a power law with an exponent  $n = \frac{4}{3}$  (dotted line, see text). The upper critical point  $B_{\text{crit,up}}$  is defined by an extrapolation to zero of the  $\Delta S$  data shown in (b). (b) Entropies of melting  $\Delta S$  and the Gaussian half-width  $\sigma$  of the respective melting transition, plotted as functions of temperature  $T$ . In the gray-shaded region,  $\Delta S$  drops significantly,  $\sigma$  increases, and the melting temperatures  $T_m$  are reduced when compared to a high-temperature fit to a power-law [see (a)].

The scaling field  $H_{m0}$  and the exponent  $n$  both depend on the microscopic mechanism that is assumed to be responsible for the melting of the vortex lattice, and on the  $T$  dependence of the Ginzburg-Landau parameters near  $T_c$ .<sup>2,3,27</sup> Below  $\mu_0 H = 5$  T, we find almost exactly  $n = \frac{4}{3}$ , which seems to be a consequence of the applicability of a three-dimensional XY scaling on approaching the critical temperature.<sup>3</sup> Near the upper-critical point ( $B_{\text{crit,up}} \approx 12$  T in our sample), where the first-order nature of the phase transition is lost, marked deviations from the power law (4) have been observed, leading to a slightly  $S$ -shaped melting line  $H_m(T)$  (Refs. 23–25) [see Fig. 2(a)]. However, in the region of applicability of Eq. (4) we may express  $T_m(\Theta)$  as

$$T_m(\Theta) = T_c \{1 - [H/f(\Theta)H_{m0}]^{1/n}\}. \quad (5)$$

We have measured the melting temperatures  $T_m(\Theta)$  for fixed magnetic fields  $\mu_0 H = 3, 5,$  and  $7.5$  T and varying  $\Theta$ . The  $T_m$  values have been obtained from fits to corresponding measured entropy increases  $\delta S(T)$  across the melting transition presented later in Sec. III B. In Fig. 3(a) we have plotted the resulting  $T_m(\Theta)$  data, together with the expectations according to Eq. (5) using  $\mu_0 H_{m0} = 110$  T,  $n = 1.35$ ,  $T_c = 92.4$  K,

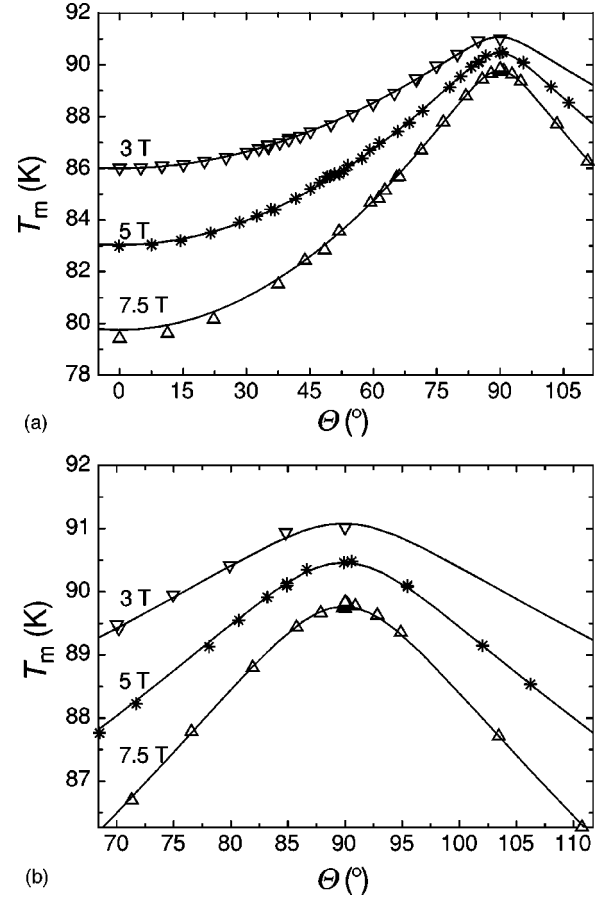


FIG. 3. (a) Melting temperatures  $T_m$  as functions of  $\Theta$ , for fixed magnetic fields  $\mu_0 H = 3, 5,$  and  $7.5$  T. The lines represent expectations according to Eq. (5) with the material parameters given in the main text. (b) Magnification of the region around  $\Theta = 90^\circ$ .

and  $\gamma = 8.28$ . Except for the parameter  $\gamma$ , these values have been independently obtained from a fit to the  $H \parallel c$  data from Fig. 2(a) below  $\mu_0 H = 5$  T according to Eq. (4). Above  $T = 82.5$  K the agreement is excellent, and there are no significant deviations in  $T_m(\Theta)$  around  $\Theta = 90^\circ$  [see Fig. 3(b)]. The systematic deviation of the  $T_m(\Theta)$  data from the result of Eq. (5) below  $T = 82.5$  K (i.e., above  $\mu_0 H \approx B_{\text{crit,up}}/2$ ) can be ascribed to the simple fact that below this temperature, the melting line does no longer follow Eq. (4). The corresponding temperatures  $T_m$  are somewhat shifted towards lower temperatures than we expect from a simple power-law behavior<sup>23–25</sup> [see Fig. 2(a)]. This apparent reduction of  $T_m$  near the upper critical point  $B_{\text{crit,up}}$  is not only observed in  $\text{YBa}_2\text{Cu}_3\text{O}_7$ , but also in  $\text{Bi}_2\text{Sr}_2\text{CaCu}_2\text{O}_8$ .<sup>10</sup> It is reasonable to assume that the vortex lattice becomes more and more susceptible to disorder on approaching  $B_{\text{crit,up}}$ , which manifests itself in an increased width of the melting transition, a reduction of the latent heat, and a slight decrease of the melting temperature [see Fig. 2(b)].

### B. The entropies of melting $\Delta S(\Theta, H)$

Within the same anisotropic scaling theory one can show that the electronic heat capacity at a given temperature  $T$  in

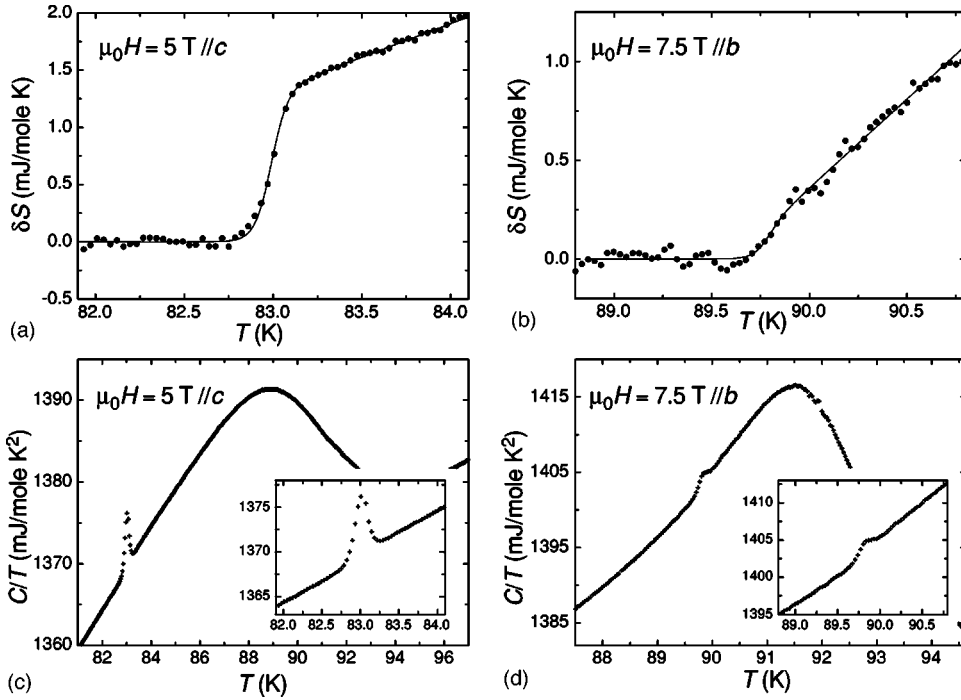


FIG. 4. Representative changes  $\delta S$  in entropy at the vortex-lattice melting transition [upper panels (a) and (b)]. A polynomial background has been subtracted for clarity (see text). The corresponding reduced heat capacities  $C/T$  are shown in the lower panels (c) and (d).

an external magnetic field  $H(\Theta)$  that is tilted away from the  $c$  axis has the same value as one would measure in a field  $H\parallel c$  that fulfills the condition<sup>30,31</sup>

$$H(\Theta) = f(\Theta)H. \quad (6)$$

This implies that at a given vortex-lattice melting temperature  $T_m$  and in any of the corresponding melting fields  $H_m(\Theta, T_m) = f(\Theta)H_{m0}(T_m)$  the latent heat  $L = T\Delta S$  should always have the same value. In other words, the entropy of melting depends only on  $T_m$ , and  $\Delta S(\Theta, H, T) = \Delta S(T)$ .<sup>21,30,31</sup> In our experiment we have first measured  $\Delta S(T)$  for  $H\parallel c$  as a reference data set, and we compare the result with the corresponding data obtained for tilted magnetic fields. If the above scaling arguments hold, all  $\Delta S(T)$  data will precisely collapse onto one single curve.

We have measured the variation in the entropies  $S$  according to similar techniques as we previously described in Ref. 9. We note here that these entropy data are virtually free of instrumental broadening on the temperature scale, because the data analysis includes a simple but efficient deconvolution procedure to account for the finite, known thermal constants of our DTA experiment.<sup>18</sup> We have obtained the  $\Delta S$  values by assuming a Gaussian broadening of the transition with a half-width  $\sigma$  centered around  $T_m$ , and by fitting the parameters  $T_m$ ,  $\sigma$ ,  $\Delta S$ , the associated broadened increase in specific heat  $\Delta C/T$ , and the coefficients for a background polynomial (typically of third order). The technical details of this data analysis will be published elsewhere. In Fig. 4 we have plotted representative entropy changes  $\delta S$  and the corresponding heat capacity  $C/T$  data, to show examples for both large and small values of  $\Delta S$ , respectively. To visualize the changes in  $S$  more clearly, we have subtracted the fitted polynomial background and obtain the  $\delta S$  data shown in Fig. 4.

In Fig. 5, we show the resulting  $\Delta S$  data in units of  $\text{mJ mole}^{-1} \text{K}^{-1}$ . The data do indeed collapse onto one single curve, with much more precision than we had observed earlier in another experiment with less resolution, where we rotated  $H$  within the  $ac$ -plane.<sup>21</sup> However, this way of representing the data is not very helpful to identify possible small deviations from anisotropic-scaling expectations, or to reveal the detailed behavior of  $\Delta S$  near  $\Theta = 90^\circ$ . Therefore, we are drawing  $\Delta S$  vs the angle  $\Theta$  in Fig. 6, where the region around  $\Theta = 90^\circ$  is of particular interest. Within the accuracy of the measurement, we do not see any discontinuous changes in  $\Delta S(\Theta)$  for  $\mu_0 H = 5$  and  $7.5$  T around  $\Theta = 90^\circ$ . This is particularly true in a window of  $\pm 0.3^\circ$  around  $90^\circ$  [see inset of Fig. 6(b)], where such changes can be expected on the basis of corresponding resistivity measurements.<sup>41</sup>

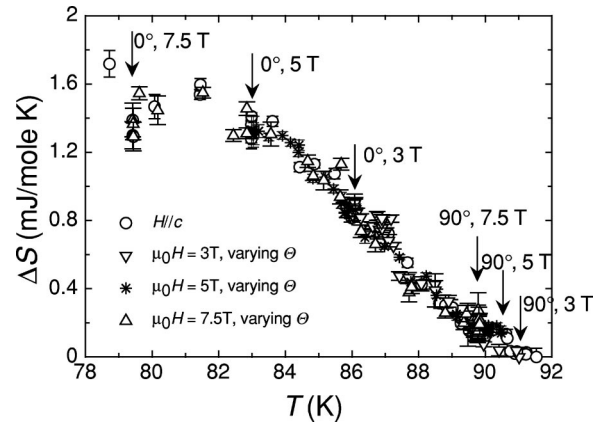


FIG. 5. Entropies of vortex-lattice melting  $\Delta S(\Theta, T)$ , for varying angles  $\Theta$  and magnetic fields  $H$ , plotted in one graph in units of  $\text{mJ mole}^{-1} \text{K}^{-1}$ . The data collapse onto one single curve. The arrows indicate the location of the data points for  $\Theta = 0^\circ$  and  $90^\circ$  for each of the considered magnetic fields.

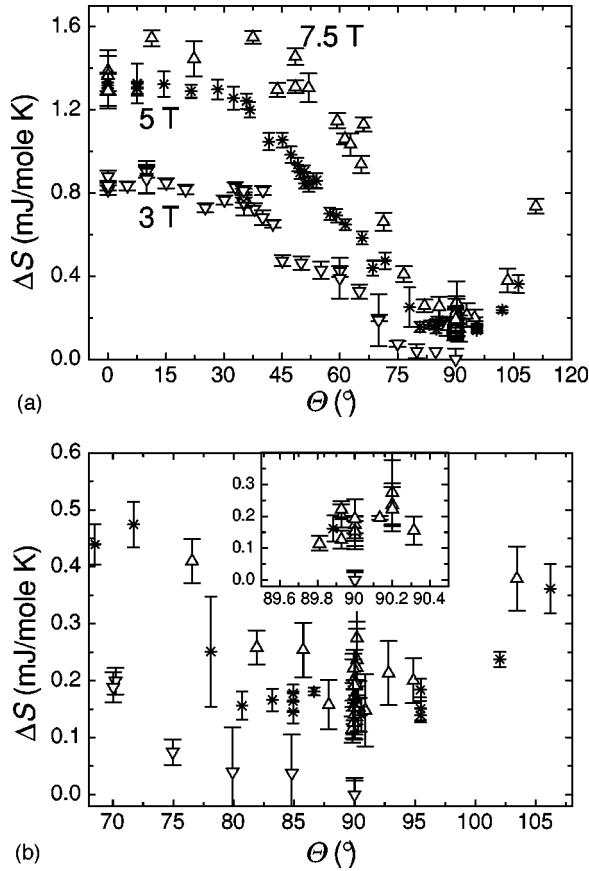


FIG. 6. (a) The same data as shown in Fig. 5 for tilted magnetic fields, plotted as functions of the angle  $\Theta$ . (b) shows a magnification of the region around  $\Theta = 90^\circ$  where  $H \parallel b$ .

Note that the apparently increased scatter in the data of Fig. 6(b) is a result of the large number of experiments that we have done around  $90^\circ$ .

There is a clear suppression of  $\Delta S(\Theta)$  for  $\mu_0 H = 3$  T, however, starting at an angle of the order of  $\Theta = 75^\circ$ , which is not observed in the data for higher magnetic fields. To decide whether or not this drop is associated with a deviation from anisotropic scaling behavior, we again have to compare the data with respective  $\Delta S$  values for  $H \parallel c$ . For this purpose we convert the data into more common dimensionless units of  $k_B$ /vortex/superconducting layer, using “normalized” magnetic-field values  $H_m(\Theta)/f(\Theta)$  that would yield the same melting temperatures  $T_m$  in a corresponding  $H \parallel c$  measurement. We have, therefore, to multiply all the  $\Delta S$  values with  $\Phi_0 s \rho f(\Theta) / M H_m(\Theta) k_B$ , where  $\Phi_0 = 2.07 \times 10^{-15}$  V s is the magnetic-flux quantum,  $s = 1.18$  nm is the interlayer distance between adjacent Cu-O double layers,  $\rho = 6380$  kg/m<sup>3</sup>, and  $M = 0.666$  kg/mole are the density and the molar weight of YBa<sub>2</sub>Cu<sub>3</sub>O<sub>7</sub>, respectively, and  $k_B = 1.38 \times 10^{-23}$  J/K is the Boltzmann constant. We realize that these dimensionless units have little physical meaning, especially for tilted magnetic fields, but they nevertheless offer a convenient way of plotting the data for the purpose of comparison.

The result of this procedure is shown in Fig. 7. Near  $T_c$ , the  $\Delta S$  data for  $H \parallel c$  show a distinct drop above  $T$

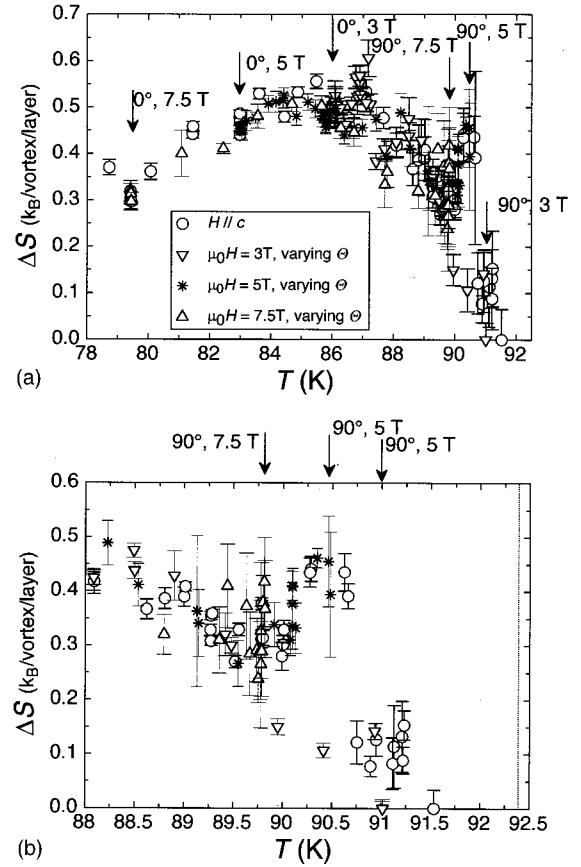


FIG. 7. (a) The data of Fig. 5, plotted in dimensionless units  $k_B$ /vortex/superconducting layer. The arrows indicate the location of the data points for  $\Theta = 0^\circ$  and  $90^\circ$  for each of the considered magnetic fields. (b) Magnification of the same data set near the critical temperature  $T_c = 92.4$  K (vertical dotted line). The entropy of melting  $\Delta S(\Theta, T)$  significantly drops at temperatures above  $T \approx 90.7$  K.

$= 90.7$  K, which is more than 1.5 K below the critical temperature. This corresponds to magnetic fields  $\mu_0 H < 0.5 T \parallel c$ . This apparent collapse of  $\Delta S(T)$  has been previously reported on the basis of magnetization<sup>15</sup> and heat-capacity data<sup>23</sup> taken on the same crystal, and we have ascribed it to the fact that a lower critical point  $B_{\text{crit,low}}$  is approached with increasing temperature.<sup>23</sup> In the present context we can suppose that this drop in  $\Delta S(T)$  near  $B_{\text{crit,low}}$  is a universal feature for our sample in the sense that the same scaling rules apply for  $B_{\text{crit,low}}$  as for all the other thermodynamic data. It should, therefore, be observable also in corresponding measurements for tilted magnetic fields as soon as  $\mu_0 H(\Theta)$  is of the order of a scaled lower critical point,  $f(\Theta)B_{\text{crit,low}}$ , and below. This is indeed what we observe for  $\mu_0 H = 3$  T above  $\Theta = 75^\circ$ , where the corresponding melting temperatures  $T_m$  are approximately in the same temperature range (i.e., above around 90 K) as the corresponding anomalous  $\Delta S(T)$  data for  $H \parallel c$ . Within this interpretation scheme, the suppression of  $\Delta S(\Theta)$  for  $\mu_0 H = 3$  T above  $\Theta = 75^\circ$  is simply a consequence of approaching the scaled lower critical point  $f(\Theta)B_{\text{crit,low}}$  from above on rotating the constant magnetic field  $H$  towards the  $b$  axis. With

$B_{\text{crit,low}} < 0.5$  T for  $H\parallel c$  and  $\gamma=8.28$ , this effect near  $H\parallel c$  can be observed only for  $\mu_0 H < 4.1$  T. Therefore, such a suppression is absent in the data for  $\mu_0 H = 5$  T and 7.5 T in Fig. 6. It is reasonable to assume that critical points of the vortex-lattice melting line scale according to Eq. (6), if the physical origin for the occurrence of these points does not impose any preferred orientation in the superconducting crystal. If the location of a critical point is mainly determined by the amount and the character of sample defects, this condition is likely to be fulfilled for a pointlike disorder, but not for line-like or planelike defects, such as, columnar tracks or twin boundaries, respectively.

#### IV. CONCLUDING REMARKS

Our present data demonstrate that the investigated  $\text{YBa}_2\text{Cu}_3\text{O}_7$  crystal does not show any anomalous behavior in its thermodynamic properties around  $\Theta = (90 \pm 0.3)^\circ$ . This is somewhat puzzling because corresponding resistivity data taken on samples of the similar origin and chemical composition show clear anomalies around  $\Theta = 90^\circ$ .<sup>41</sup> After completing our experiments we have become aware of a recent theoretical work by Hu and Tachiki,<sup>44</sup> and an extended experimental investigation by Gordeev *et al.*<sup>42</sup> According to these results it is likely that the first-order nature of the VLM transition for  $\Theta = 90^\circ$  persists, within the validity of anisotropic scaling, up to a limiting flux density, above which the intervortex spacing normal to the layers starts accommodat-

ing the period of the layered structure of the material, i.e., becomes an integer multiple  $n$  of the distance  $s$  between adjacent Cu-O double layers. This happens around

$$B \approx \frac{\sqrt{3}\phi_0}{2\gamma(ns)^2}. \quad (7)$$

For  $n=1$ , the vortex-lattice geometry is entirely dictated by the layered structure of the material, and no conventional first-order melting transition can be expected.<sup>44</sup> The transport measurements from Ref. 42 indicate, however, that this effect becomes already important for  $n=4$ . For the present crystal, this would be relevant above  $\mu_0 H \approx 10$  T, which is outside our experimental possibilities. Nevertheless, resistivity data from oxygen-depleted  $\text{YBa}_2\text{Cu}_3\text{O}_7$  with a larger anisotropy ratio  $\gamma$  indicate a distinct deviation from conventional scaling behavior of the vortex-lattice phase transition line  $H_m(\Theta, T)$  near  $\Theta = 90^\circ$  at magnetic fields well below 10 T,<sup>42</sup> which makes it attractive to repeat such heat-capacity measurements on oxygen-depleted  $\text{YBa}_2\text{Cu}_3\text{O}_7$  samples.

#### ACKNOWLEDGMENTS

This work was supported by the Schweizerische Nationalfonds zur Förderung der Wissenschaftlichen Forschung, Grant No. 2024-061943 (A.S.). The U.S. Department of Energy, BES-Materials Science, supported the work at Argonne under Contract No. W-31-109-ENG-38 (U.W., W.K.K., G.W.C.).

- 
- <sup>1</sup>D. R. Nelson, Phys. Rev. Lett. **60**, 1973 (1988).  
<sup>2</sup>A. Houghton, R. A. Pelcovits, and A. Subdø, Phys. Rev. B **40**, 6763 (1989).  
<sup>3</sup>D. S. Fisher, M. P. A. Fisher, and D. A. Huse, Phys. Rev. B **43**, 130 (1991).  
<sup>4</sup>R. G. Beck, D. E. Farrell, J. P. Rice, D. M. Ginsberg, and V. G. Kogan, Phys. Rev. Lett. **68**, 1594 (1992).  
<sup>5</sup>H. Safar, P. L. Gammel, D. A. Huse, D. J. Bishop, J. P. Rice, and D. M. Ginsberg, Phys. Rev. Lett. **69**, 824 (1992).  
<sup>6</sup>W. K. Kwok, S. Fleshler, U. Welp, V. M. Vinokur, J. Downey, G. W. Crabtree, and M. M. Miller, Phys. Rev. Lett. **69**, 3370 (1992).  
<sup>7</sup>H. Pastoriza, M. F. Goffman, A. Arribère, and F. de la Cruz, Phys. Rev. Lett. **72**, 2951 (1992).  
<sup>8</sup>R. E. Hetzel, A. Sudbø, and D. A. Huse, Phys. Rev. Lett. **69**, 518 (1992).  
<sup>9</sup>A. Schilling and O. Jeandupeux, Phys. Rev. B **52**, 9714 (1995).  
<sup>10</sup>E. Zeldov, D. Majer, M. Konczykowski, V. B. Geshkenbein, V. M. Vinokur, and H. Shtrikman, Nature (London) **375**, 373 (1995).  
<sup>11</sup>A. Schilling, O. Jeandupeux, C. Wälti, H. R. Ott, and A. van Otterloo, in *Proceedings of the 10th Anniversary HTS Workshop on Physics, Materials and Applications, Houston, 1996*, edited by B. Batlogg, C. W. Chu, W. K. Chu, D. U. Gubser, and K. A. Müller (World Scientific, Singapore), pp. 349–352.  
<sup>12</sup>R. Liang, D. A. Bonn, and W. N. Hardy, Phys. Rev. Lett. **76**, 835 (1996).  
<sup>13</sup>U. Welp, J. A. Fendrich, W. K. Kwok, G. W. Crabtree, and B. W. Veal, Phys. Rev. Lett. **76**, 4809 (1996).  
<sup>14</sup>M. Roulin, A. Junod, and E. Walker, Science **273**, 1210 (1996).  
<sup>15</sup>A. Schilling, R. A. Fisher, N. E. Phillips, U. Welp, D. Dasgupta, W. K. Kwok, and G. W. Crabtree, Nature (London) **382**, 791 (1996).  
<sup>16</sup>M. Roulin, A. Junod, A. Erb, and E. Walker, J. Low Temp. Phys. **105**, 1099 (1996).  
<sup>17</sup>A. Junod, M. Roulin, J.-Y. Genoud, B. Revaz, A. Erb, and E. Walker, Physica C **275**, 245 (1997).  
<sup>18</sup>A. Schilling, R. A. Fisher, N. E. Phillips, U. Welp, W. K. Kwok, and G. W. Crabtree, Physica C **282–287**, 327 (1997).  
<sup>19</sup>A. Schilling, R. A. Fisher, N. E. Phillips, U. Welp, W. K. Kwok, and G. W. Crabtree, Phys. Rev. Lett. **78**, 4833 (1997).  
<sup>20</sup>M. Roulin, A. Junod, A. Erb, and E. Walker, Phys. Rev. Lett. **80**, 1722 (1998).  
<sup>21</sup>A. Schilling, R. A. Fisher, N. E. Phillips, U. Welp, W. K. Kwok, and G. W. Crabtree, Phys. Rev. B **58**, 11 157 (1998).  
<sup>22</sup>M. Willemin, A. Schilling, H. Keller, C. Rossel, J. Hofer, U. Welp, W. K. Kwok, R. J. Olsson, and G. W. Crabtree, Phys. Rev. Lett. **81**, 4236 (1998).  
<sup>23</sup>A. Schilling, M. Willemin, C. Rossel, H. Keller, R. A. Fisher, N. E. Phillips, U. Welp, W. K. Kwok, R. J. Olsson, and G. W. Crabtree, Phys. Rev. B **61**, 3592 (2000).  
<sup>24</sup>C. Marcenat, Thesis of habilitation, Univ. Grenoble 1 (2000).  
<sup>25</sup>F. Bouquet, C. Marcenat, E. Steep, R. Calemczuk, W. K. Kwok, U. Welp, G. W. Crabtree, R. A. Fisher, N. E. Phillips, and A. Schilling, Nature (London) **411**, 448 (2001).

- <sup>26</sup>G. Blatter, V. Geshkenbein, A. Larkin, and H. Nordborg, *Phys. Rev. B* **54**, 72 (1996).
- <sup>27</sup>G. Blatter, M. V. Feigel'man, V. B. Geshkenbein, A. I. Larkin, and V. M. Vinokur, *Rev. Mod. Phys.* **66**, 1125 (1994).
- <sup>28</sup>H. Safar, P. L. Gammel, D. A. Huse, D. J. Bishop, W. C. Lee, J. Giapintzakis, and D. M. Ginsberg, *Phys. Rev. Lett.* **70**, 3800 (1993).
- <sup>29</sup>M. J. W. Dodgson, V. B. Geshkenbein, H. Nordborg, and G. Blatter, *Phys. Rev. Lett.* **80**, 837 (1998).
- <sup>30</sup>M. J. W. Dodgson, V. B. Geshkenbein, H. Nordborg, and G. Blatter, *Phys. Rev. B* **57**, 14 498 (1998).
- <sup>31</sup>G. Blatter, V. B. Geshkenbein, and A. I. Larkin, *Phys. Rev. Lett.* **68**, 875 (1992).
- <sup>32</sup>S. Ooi, T. Shibauchi, N. Okuda, and T. Tamegai, *Phys. Rev. Lett.* **82**, 4308 (1999).
- <sup>33</sup>A. E. Koshelev, *Phys. Rev. Lett.* **83**, 187 (1999).
- <sup>34</sup>B. I. Ivlev, Yu. N. Ovchinnikov, and V. L. Pokrovski, *Mod. Phys. Lett. B* **5**, 73 (1991).
- <sup>35</sup>L. N. Bulaevskii and J. R. Clem, *Phys. Rev. B* **44**, 10 234 (1991).
- <sup>36</sup>L. N. Bulaevskii, M. Ledvij, and V. G. Kogan, *Phys. Rev. B* **46**, 366 (1992).
- <sup>37</sup>B. I. Ivlev and L. J. Campbell, *Phys. Rev. B* **47**, 14 514 (1992).
- <sup>38</sup>L. Balents and D. R. Nelson, *Phys. Rev. Lett.* **73**, 2618 (1994).
- <sup>39</sup>L. Balents and D. R. Nelson, *Phys. Rev. B* **52**, 12 951 (1995).
- <sup>40</sup>X. Hu and M. Tachiki, *Phys. Rev. Lett.* **80**, 4044 (1998).
- <sup>41</sup>W. K. Kwok, U. Welp, V. M. Vinokur, S. Fleshler, J. Downey, and G. W. Crabtree, *Phys. Rev. Lett.* **67**, 390 (1991).
- <sup>42</sup>S. N. Gordeev, A. A. Zhukov, P. A. J. de Groot, A. G. M. Jansen, R. Gagnon, and L. Taillefer, *Phys. Rev. Lett.* **85**, 4594 (2000).
- <sup>43</sup>L. J. Campbell, M. M. Doria, and V. G. Kogan, *Phys. Rev. B* **38**, 2439 (1988).
- <sup>44</sup>X. Hu and M. Tachiki, *Phys. Rev. Lett.* **85**, 2577 (2000).